IJST, Transactions of Mechanical Engineering, Vol. 39, No. M1, pp 77-87
Printed in The Islamic Republic of Iran, 2015
© Shiraz University

AN EXPERIMENTAL AND NUMERICAL STUDY OF DUCTILE FRACTURE OF COPPER/STAINLESS STEEL CLAD SHEET IN DEEP DRAWING PROCESS[*]

M. MASHAYEKHI[**], F. DEHGHANI, N. TORABIAN AND M. SALIMI

Dept. of Mechanical Engineering, Isfahan University of Technology, Isfahan 84156-83111, I. R. of Iran
Email: mashayekhi@cc.iut.ac.ir

Abstract– This work is an attempt towards employing ductile damage criterion and finite element simulations for prediction of fracture initiation and evolution in deep drawing of copper/stainless steel clad sheets. The material mechanical properties and ductile damage parameters were determined through standard and notched tensile tests. The effect of some important process parameters on damage evolution were examined through numerical modeling and the acceptable range of variations for each parameter were introduced in order to prevent tearing of the blank during the process. The numerical predictions of deformation and fracture behavior were in a good agreement with experimental observations.

Keywords– Copper/stainless steel clad sheet, ductile damage, deep drawing

1. INTRODUCTION

In recent years, due to the considerable demands of modern industries for multi-functional products, clad sheet metals have been increasingly used in various fields such as automobile, aerospace and electrical industries, because of their excellent mechanical and functional properties. Moreover, by virtue of good corrosion resistance, clad plates have been increasingly used in both chemical and petroleum industries.

Binding two discrete materials with different physical and mechanical features can be done by either fusion or solid state welding. In solid state welding, joining of two surfaces takes place by atomic bonding between the atoms on the surfaces and it can be done via various processes such as roll bonding, explosive welding, friction welding, ultrasonic welding and laser forming [1].

Explosive welding, which works by means of detonation energy, can be used to join similar or dissimilar metals that cannot be joined by other welding or bonding techniques. In this process, controlled explosive detonations are used to accelerate one or both of the constituent metals into each other in such a manner as to cause the collision to fuse them together. In explosive welding process, a flyer plate is supported parallel or at an oblique angle to a base plate. The flyer plate is covered by a buffer which may be made of a thin rubber sheet. The explosive is then placed on top of the buffer sheet. Following the explosion, the flying plate collapses to the base plate and a metallic jet is formed at the impingement line between the two plates. The high velocity oblique collision will produce high pressure, high temperature and high shear strain near the collision point in a very short time. The bond is generally wavy with a good tensile strength because of the large and wavy contact surface.

Among different forming processes, deep drawing is a familiar method of forming clad metal sheets. In the open literature, deep drawing of clad sheets has been investigated from different aspects. Rees and Power [2] determined a forming limit diagram for a zinc-clad rolled steel sheet. They revealed how the

formability of the materials is influenced by their composition, thickness, strain path, lubrication and heat treatment. Tukuda and Htla [3] predicted the formability of the aluminum 2024 sheet and its laminates clad by mild steel sheets through finite element simulation of axisymmetric deep drawing process. Parsa et al. [4] investigated the deep drawing and redrawing characteristics of a two-layer stainless steel/aluminum sheet by numerical simulations and experiments. They showed that the setting condition has an important effect on the specimen behavior during deep drawing and redrawing processes. Tseng et al. [5] predicted the fracture and the formability of Al/Cu clad metal sheets by finite element simulations as well as deep drawing tests. They showed that the formability of clad metal sheets can be manipulated by changing the process parameters such as the holding force and the blank diameter. Padmanabhan et al. [6] investigated the deep drawing of aluminum/steel tailor welded blanks and showed that by using a lower blank holder force on the higher strength material side, the tendency of tearing in the weaker material can be reduced. Bosh et al. [7] developed a numerical model to predict the delamination of the polymer coating from the steel substrate during deep drawing process. Morovati et al. [8] investigated the wrinkling of two-layer aluminum/stainless steel sheets in the deep drawing process through analytical methods, numerical simulations, and experiments. They obtained the minimum required blank holder force to prevent wrinkling.

One of the applications of copper/stainless steel clad sheets is in the production of expansion valves manufactured by deep drawing where the material of the interior is copper and the exterior is stainless steel; since the thermal conductivity of steel is lower than that of copper, the energy lost in expansion valves would be decreased by using these clad sheets.

In the present work, finite element numerical simulations coupled with ductile damage criterion were employed to investigate fracture initiation and evolution during deep drawing of stainless steel/copper clad sheets; stainless steel and copper plates were bonded through explosive welding process. Afterwards, the mechanical properties of the produced clad metal sheets were measured by tensile tests. After that, deep drawing of the sheets with different values of initial blank diameter was carried out. The deep drawing tests were also simulated with finite element method (FEM) and the ductile damage model was employed in order to predict the tendency of blank tearing during the process. The material damage parameters were obtained from tensile tests on flat-grooved specimens. The accuracy of the FE model was verified by comparing the numerical results with experimental observations. Finally, the effects of some process parameters on damage evolution and fracture initiation during the deep drawing process were inspected.

2. EXPERIMENTAL PROCEDURE

Explosive welding was carried out for bounding stainless steel and copper plates as follows: Austenitic stainless steel 304L was chosen as the base plate with dimensions of 420×520×1 mm, while copper was used as the flyer plate with dimensions of 420×520×1 mm. The chemical compositions and mechanical properties of the materials were determined through experiments and are presented in Tables 1 and 2, respectively. Amatol (TNT 10% and ammonium nitrate 90%) was used as the explosive material. The initial gap between two metal plates was chosen to be about 3 mm. The matching surfaces were carefully cleaned by polishing and degreaser. After welding, in order to avoid formation of $Cr_{23}C_6$ in stainless steel, post heat treatment process was performed at 300°C for 32 hours.

Table 1. The chemical composition of stainless steel 304L and copper

Elements (wt.%)	Cr	Ni	Mn	C	Si	S	Al	Cu	Fe
AISI 304L (base plate)	18.91	8.44	1.79	0.015	0.483	0.03	–	0.043	Balanced
Copper (flyer plate)	0.03	0.03	–	–	–	–	0.155	Balanced	0.05

Table 2. The mechanical properties of stainless steel 304L and copper

Material	R_0 (RD)	R_{45} (DD)	R_{90} (TD)	Tensile Strength (MPa)
Stainless Steel	1.215	1.327	1.24	298
Copper	0.763	0.767	0.762	78

Figure 1 illustrates Optical Microscopy (OM) graphs of copper/stainless steel joints after heat treatment; it is clear that the bonding at the copper/steel interface has wavy morphology which gives rise to improve the joint quality [9, 10]. Moreover, there was no melting zone in the welded interface and it is due to the proper selection of the welding parameters. In addition, in order to assess the joint quality and the possibility of imperfection existence in the interface peeling tests were performed according to ASTM-D1876-72 standard. The dimensions of the test specimens were prepared according to the ASTM-D1876 standard and the results are illustrated in Fig. 2. According to these results, the strength of the bond between the copper and the steel is equal to or greater than the strength of the copper itself.
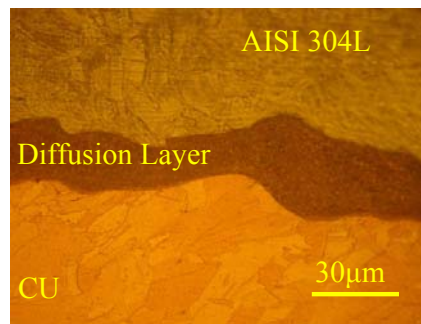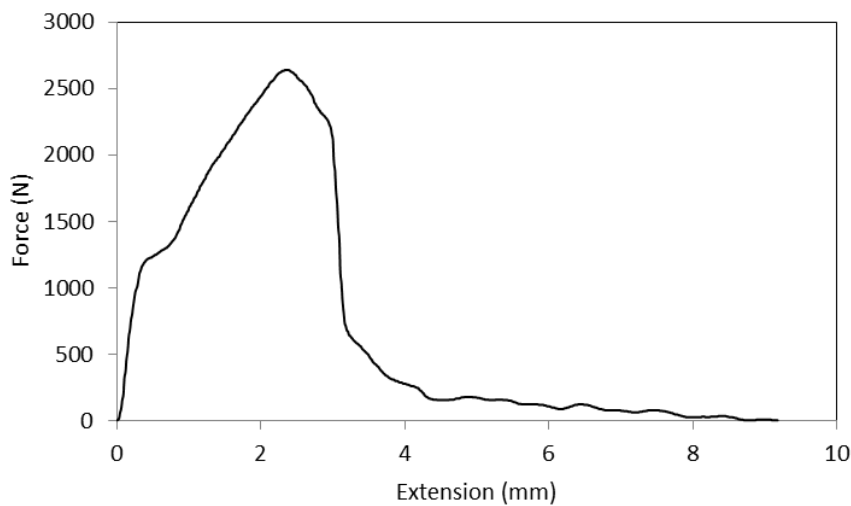

Fig. 1. OM picture of copper/steel joint after heat treatment

(a)

(b)

Fig. 2. (a) Peeling test sample (b) The peeling force versus the peeling distance

Moreover, according to Fig. 2, the deformation behavior is homogeneous, indicating a ductile behavior of the joint which prevents brittle fracture occurrence. Therefore, based on the iso-strain deformation behaviors of copper/stainless steel clad metal sheets, in the numerical modeling these sheets can be considered to be equivalent to a single layer with the material parameters of copper/stainless steel clad sheet [5].

In order to measure the mechanical behavior of the produced copper/stainless steel clad sheet, tensile tests were carried out on a Hounsfield testing machine. Standard tensile specimens were selected according to ASTM E8M04 and the rate of displacement was adjusted to 5 mm/min. Three specimens were manufactured and tested and the results of the three tests were averaged to obtain the stress-strain diagram as shown in Fig. 3. Furthermore, the Lankford coefficients of the clad sheet were measured through experiments as presented in Table 3.
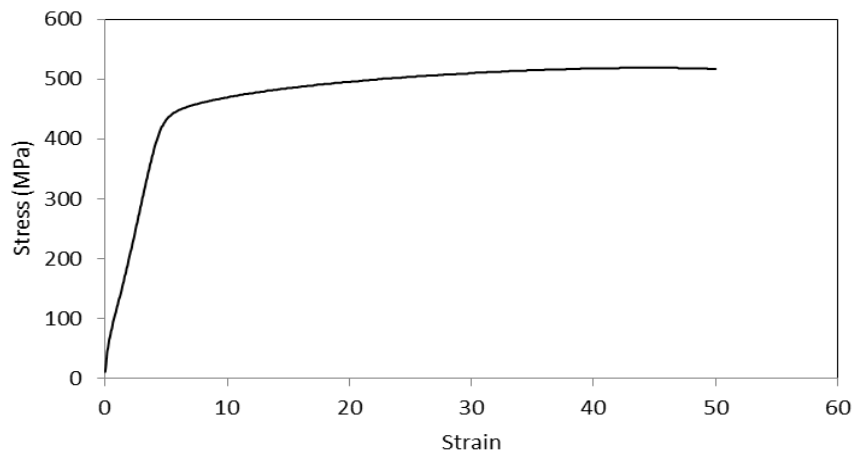

Fig. 3. Stress-strain curve of the copper/steel clad sheet

Table 3. The anisotropy coefficients of the copper/stainless steel clad sheet

R_0 (RD)	R_{45} (DD)	R_{90} (TD)
0.766	1.247	1.461

3. DEEP DRAWING PROCESS

In deep drawing process the sheet is pushed into the matrix by moving the punch, whereas the blank holder controls the sheet flow during the process. The dominant process parameters are the blank holder pressure, the clearance between the punch and the matrix, the friction condition and the initial blank shape which should be properly determined and controlled in order to maintain high levels of product quality and productivity. Moreover, deep drawing of two different materials simultaneously, as in the case of clad sheet forming, requires special consideration because of the high differences in the materials mechanical properties.

Generally, the two dominant modes of failure in sheet metal deep drawing are wrinkling and tearing. Additionally, earring is another defect in deep-drawn products which stems from the anisotropic characteristics of the workpiece. In this study, tearing of the blank is predicted and investigated by employing ductile damage criterion which is a powerful tool in prediction of material failure during forming processes.

In the present work, deep drawing tests were performed using a 160 ton hydraulic press. Circular clad sheet samples with initial diameters of 100, 105, 110 and 115 mm were prepared; each diameter results in

a specific drawing ratio. The copper side of the copper/stainless steel clad sheets was in contact with the punch. The geometrical characteristics of the testing setup are presented in Table 4.

Table 4. The properties of the deep drawing testing machine

Punch diameter, D_p(mm)	Die diameter, D_d(mm)	Punch edge radius (mm)	Die edge radius (mm)	Blank holder pressure (MPa)	Thickness (mm)	
					Steel	Copper
50	54.56	10	10	0.875	0.95	0.95

4. DUCTILE DAMAGE MODEL

Generally speaking, product defects in metal forming processes can be addressed by employing two different categories of approaches. The first category, which is referred to as the traditional approach, consists of stress-and-strain based methods and traditional fracture mechanics. Although this type of approach has been widely used in the literature, it had some limitations in predicting fracture initiation [11-14]. The second type of approach, ductile damage criterion, is a powerful tool in prediction of material failure which has been successfully employed in different forming processes including deep drawing [15].

In this paper, for prediction of tearing of the blank, the ductile damage model proposed by Hooputra et al. [16] is employed in this study. In this model, it is assumed that the equivalent fracture strain, $\overline{\varepsilon}_f$, is a function of stress triaxiality, η, in the form of Eq. (1) [16]:

$$\overline{\varepsilon}_f = d_1 \exp(-c\eta) + d_2 \exp(c\eta) \tag{1}$$

where d_1, d_2 and c are material parameters which should be determined through experiments. Also, η is defined in Eq. (2):

$$\eta = \frac{\sigma_H}{\sigma_{eq}} \tag{2}$$

in which σ_H is the hydrostatic stress and $\sigma_{eq} = \sqrt{\frac{3}{2}\sigma_{ij}^D \sigma_{ij}^D}$ is the Misses equivalent stress. According to ductile damage model, the damage parameter is defined as:

$$D = \int_0^{\overline{\varepsilon}_f} \frac{d\overline{\varepsilon}}{\overline{\varepsilon}_f(\eta)} \tag{3}$$

Moreover, the fracture criterion is met when D is equal to a critical value, D_{cr}.

In this study, the material damage parameters were determined according to the experimental procedure proposed by Bai et al. [17]; flat-grooved tensile specimens were used to investigate the effect of stress triaxiality on fracture strain. Figure 4 shows a flat-grooved specimen from both copper and steel side views. The thickness of the specimen at the groove is represented by t and the radius of the groove is R. The groove causes stress concentration at the center of the specimen and different values of groove radii give rise to different values of stress triaxiality [17]. In order to determine the material damage parameters, three specimens with groove radii of 4, 6 and 12 mm were designed and manufactured from the produced copper/ stainless steel clad sheet. The stress triaxiality at the center of the specimen is given by the modified Bridgman equation as follows [17]:

$$\eta = \frac{\sqrt{3}}{3}[1 + 2\ln(1 + \frac{t}{4R})] \tag{4}$$

where t is the ligament thickness of the specimen and R is the groove radius. Moreover, the equivalent strain to fracture in the necking cross section of a flat-grooved specimen can be approximately determined using the logarithmic measure of strain [17]:

$$\overline{\varepsilon}_f = \frac{2}{\sqrt{3}}\ln(\frac{t_0}{t_f}) \tag{5}$$

where t_0 and t_f are the initial and fracture ligament thicknesses of the specimen, respectively. This formula defines the average strain through the cross section.

Fig. 4.The flat grooved specimen of copper/stainless steel clad sheet for
determining the material damage parameters

Tensile tests were performed on the grooved specimens and the ligament thickness of each specimen was measured after fracture. The test results are summarized in Table 5.

According to the results presented in Table 5, the material damage parameters in Equation (1) can be obtained through curve fitting, as presented in Table 6.

Table 5. The results of the tensile tests on the flat-grooved specimens

Groove radius (mm)	initial thickness, t_0 (mm)	Final thickness, t_f (mm)	Stress triaxiality, η	Equivalent fracture strain, $\overline{\varepsilon}_f$
4	0.95	0.87	0.6439	0.10158
6	0.95	0.62	0.6222	0.49276
12	0.95	0.55	0.5998	0.63109

Table 6. The ductile damage parameters for copper/stainless steel clad sheet

d_1	d_2	c	D_{cr}
19.53	-16.91	0.09827	0.8

5. NUMERICAL SIMULATIONS OF THE DEEP DRAWING PROCESS

In this section, the fracture prediction of copper/stainless steel clad sheets during deep drawing process is carried out and verified through finite element simulations. The deep drawing test introduced in Section3 was modeled using ABAQUS/Explicit commercial software. In this case a 1/4 symmetric model was used. The copper/stainless steel was considered as an equivalent single layer material [5], with material parameters previously determined from tensile tests of copper/stainless steel clad sheets. The blank was meshed with linear hexahedral elements of type C3D8R while the die, punch, and holder were considered to be discrete rigid bodies. According to experimental data, the Coulomb coefficient of friction was set to

0.05 for the blank-die contact, 0.07 for the blank-holder contact, and 0.15 for other contact surfaces. In addition, an equivalent pressure of 0.875 MPa was applied on the blank through the holder.

The thickness distribution obtained from the numerical simulations is compared to the experimental results in Fig. 5. It is clear that there is a good agreement between the numerical predictions and experimental observations.
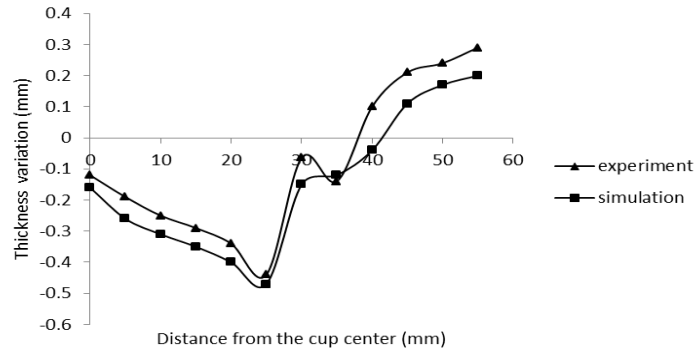

Fig. 5. Experimental and numerical thickness distribution

For fracture prediction, the ductile damage criterion option was used, based on the damage parameters presented in Table 6. The simulations were carried out for two different drawing ratios of 2.2 and 2.3 (which correspond to the blank initial diameters of 110 and 115 respectively). The simulation results for damage evolution through the sheet are compared to the experimental observations in Fig. 6.
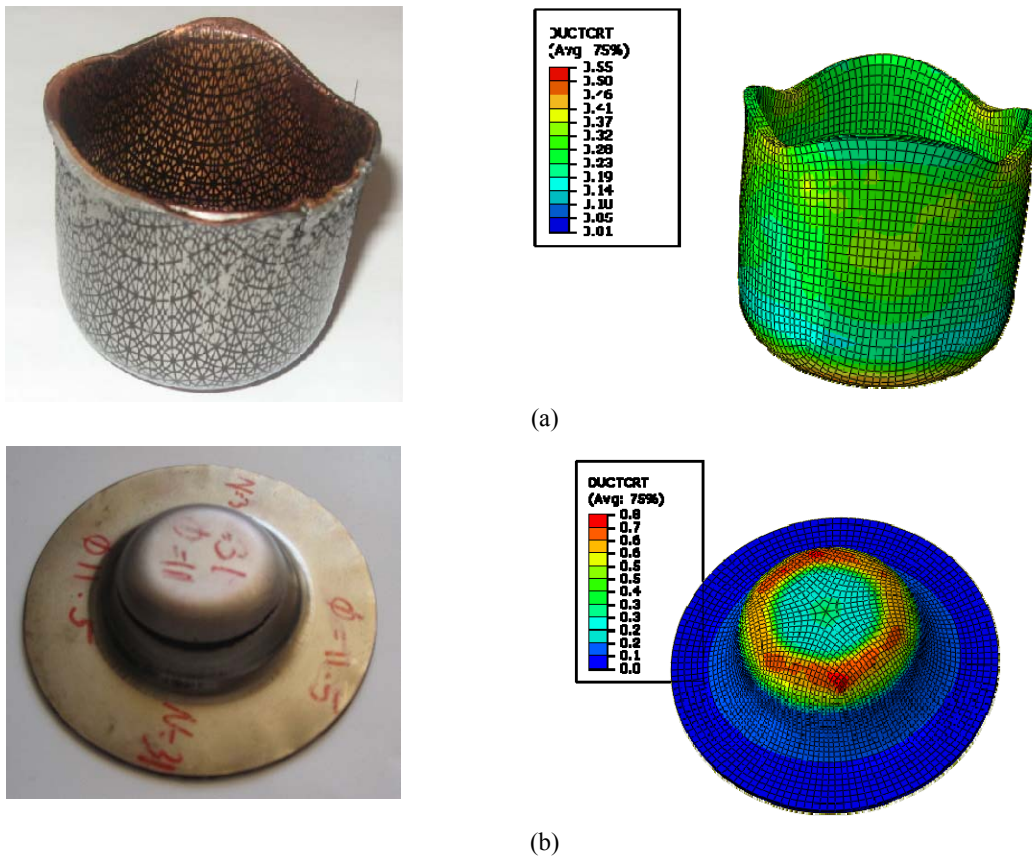

(a)

(b)

Fig. 6. Experimental and numerical results for (a) $r = 2.2$ (b) $r = 2.3$

By comparison of the numerical predictions with the experimental observations (Figs. 6-b) the critical damage value was set to $D_{cr} = 0.8$, therefore, it is clear that for $r = 2.2$ no tearing occurs while for $r = 2.3$ tearing was predicted to occur at the top corner of the blank with a drawing depth of 30 mm and this is in accordance with the experimental results. Moreover, it can be seen from Fig. 6a that according to the numerical results the anisotropy of the clad sheet causes earring in the final product which is in a good agreement with the experimental observations.

In the following sections, the damage coupled finite element model will be employed to investigate the effect of different process parameters on damage evolution and tearing of the blank.

6. EFFECT OF PROCESS PARAMETERS ON DAMAGE EVOLUTION THROUGH THE BLANK

In general, some of the dominant parameters of a deep drawing process are friction coefficients, blank holder pressure, and the die and punch edge radii. In this section the effects of these parameters on fracture initiations during the deep drawing of copper/steel clad sheets are investigated via finite element simulations.

a) Effect of friction conditions

Generally, three contact surfaces can be considered: blank-die, blank-punch, and blank-holder contacts. The damage evolution through the blank was investigated for different values of friction coefficient at these contact surfaces through finite element simulations and the results are presented in Fig. 7. From Fig. 7a it is clear that the friction coefficient at the blank-die contact, f_d, surface plays an important role in damage evolution, as by increasing f_d, the maximum damage value increases considerably and for $f_d = 0.1$, the maximum damage parameter reaches its critical value, $D_{\max} = 0.8$.

Moreover, as can be seen from Fig. 7b, the variation of the friction coefficient at the blank-holder contact surface, f_b, affects the damage value and in order for the damage parameter to remain under the critical value, f_b should meet the criterion $f_b \leq 0.35$.

However, Fig. 7c shows that the blank-punch contact friction coefficient, f_p, does not influence the damage value and $D_{\max}$ remains roughly the same (around 0.58) for $0.1 \leq f_p \leq 0.7$. Therefore, f_p cannot be considered as an effective factor for tearing of the clad metal blank during the deep drawing.

The obtained numerical results are compatible with the physical nature of the process; from the physical point of view, the relative motion between blank and die as well as that of blank and holder are considerable, which makes the friction an effective factor for these two sets of contact, while the opposite is true for the blank-punch contact.
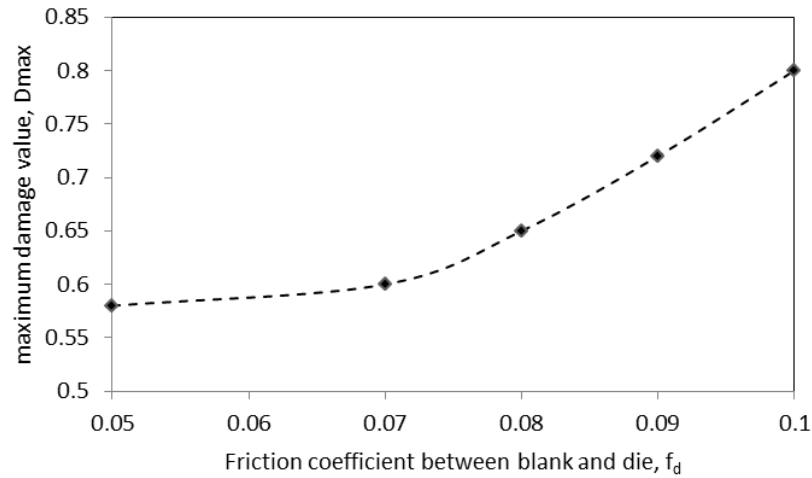
b) Effect of blank holder pressure

Numerical simulations were carried out for different values of blank holder pressure and the results are presented in Fig. 8. This figure shows that the maximum damage value increases along with an increase in the pressure until it reaches its critical value, $D_{\max} = 0.8$ for $P = 3$ MPa. These numerical predictions are compatible with experimental observations, as for the pressure range of 1.3 MPa $\leq P \leq 2.2$ MPa, no blank tearing was detected in practice.
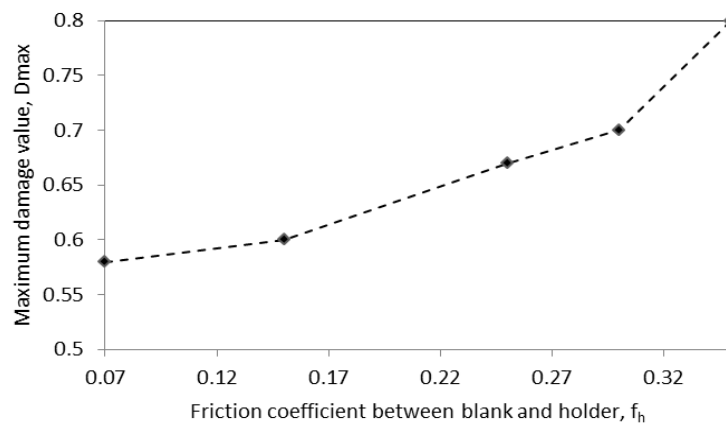
c) Effect of die and punch edge radii

Finite element simulations were performed for four different edge radius values of 11, 13, 14 and 15 mm and the results indicate that this parameter does not affect damage evolution and consequently tearing of the blank, as the maximum damage parameter remains around 0.6 for all cases (Fig. 9). From the
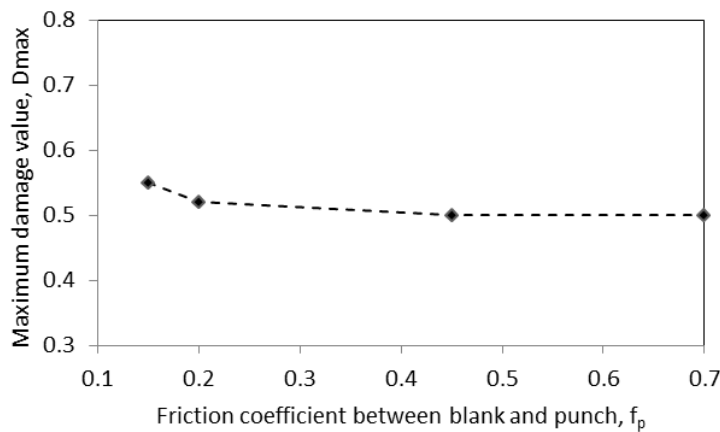
physical point of view this result stems from the ignorable contact between the blank and the die and punch corners during the process.

(a)

(b)

(c)

Fig. 7. Variations of maximum damage value versus the friction coefficient at the contact surface of (a) blank-die (b) blank-holder (c) blank-punch
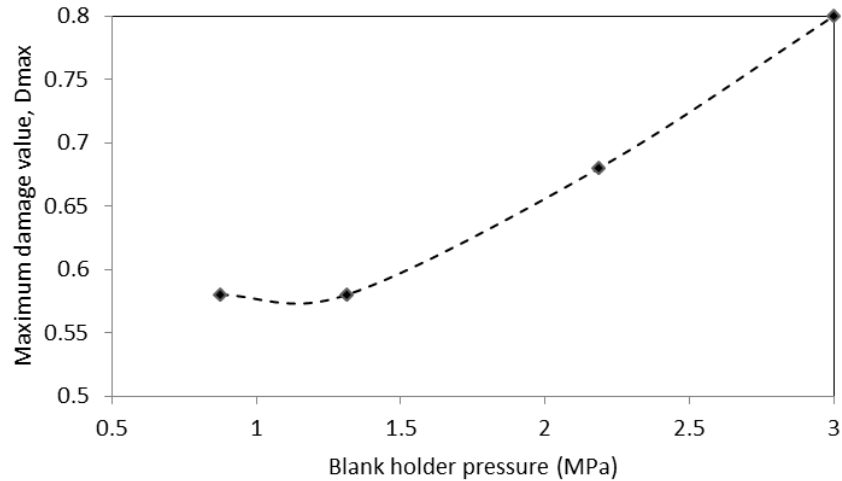
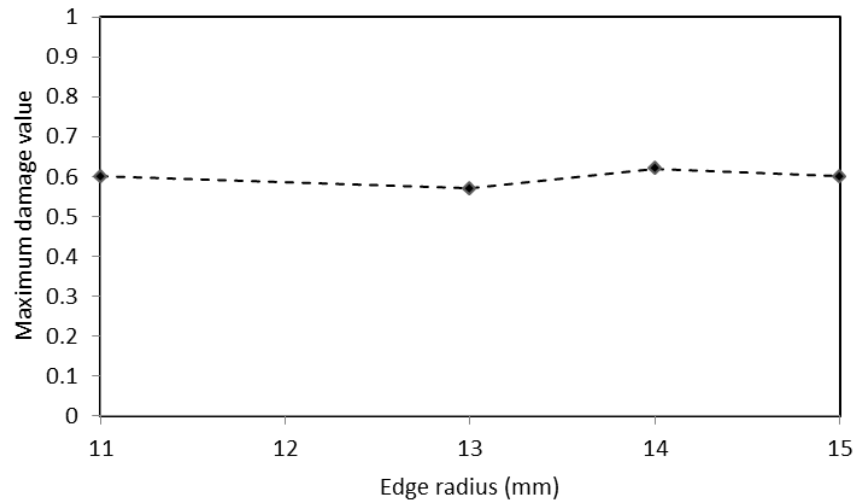Fig. 8. Variations of maximum damage parameter versus pressure

Fig. 9.Variations of maximum damage parameter versus edge radius value

7. CONCLUSION

In this research, the applicability of ductile damage criterion coupled with finite element analysis for fracture prediction in deep drawing of copper/stainless steel clad sheets produced by explosive welding was examined. The mechanical properties and material damage parameters were obtained from experiments. The capability of the ductile damage model incorporated in a FE code for prediction of fracture initiations and evolution was verified by experimental observations. In addition, the thickness distribution and deformation behavior of the clad sheet, including the earring phenomenon, were accurately predicted by the developed FE code. The experiments showed that there is no considerable difference between the formability of the copper/stainless steel clad sheets and the formability of the single layer copper and steel sheets. Moreover, the results of this research show that the formability of copper/stainless steel clad metal sheets can be manipulated by changing some of the deep drawing process parameters such as the contacts friction conditions and the holding pressure; it was observed that the friction coefficient at the blank-die contact and blank-holder contact as well as the pressure have a

significant effect on damage growth during the process. However, the friction condition at the blank-punch contact as well as the edge radius of die and punch do not affect damage and fracture of the specimens.

REFERENCES

1. Kahrman, N., Gulenc, B. & Findik, F. (2005). Joining of titanium/stainless steel by explosive welding and effect on interface. *J. Mate. Process. Technol*., Vol.169, pp. 127-133.
2. Rees, D. W.A. & Power, R. K. (1994). Forming limits in a clad steel. *J. Mater. Process. Technol*., Vol. 45, pp. 571-575.
3. Takuda, H. & Hatta, N. (1998). Numerical analysis of the formability of an aluminum 2024 alloy sheet and its laminates with steel sheets. *Metall. Mater. Trans. A*., Vol. 29, pp. 2829-2834.
4. Parsa, M. H., Yamaguchi, K. & Takakura, N. (2001). Redrawing analysis of aluminum–stainless-steel laminatedsheet using FEM simulations and experiments. *Int. J. Mech. Sci*., Vol. 43, pp. 2331–2347.
5. Tseng, H. C., Hung, C. & Hung, C. C. (2010). An analysis of the formability of aluminum/copper cladmetals with different thicknesses by the finite Element method and experiment. *Int. J. Adv. Manuf. Technol*., Vol. 49, pp. 1029-1036.
6. Padmanabhan, R., Oliveira, M. C. & Menezes, L. F. (2008). Deep drawing of aluminium–steel tailor-welded blanks. *Mater. Design*, Vol. 29, pp. 154–160.
7. van den Bosch, M. J., Schreursa, P. J. G. & Geers, M. G. D. (2009). On the prediction of delamination during deep-drawing of polymer coated metal sheet. *J. Mater. Process. Tech*., Vol. 209, pp. 297–302.
8. Morovvati, M. R., Fatemi, A. & Sadighi, M. (2011). Experimental and finite element investigation on wrinkling of circular single layer and two-layer sheet metals in deep drawing process. *Int. J. Adv. Manuf. Tech*., Vol. 54, pp. 113-121.
9. Findik, F. (2011). Recent developments in explosive welding. *Mater. Design*, Vol. 32, pp. 1081–93.
10. Durgutlu, A., Gulenc, B. & Findik, F. (2005). Examination of copper/stainless steel joints formed by explosive welding. *Mater. Design*, Vol. 26, pp. 497–507.
11. Saanouni, K., Badreddine, H. & Ajmal, M. (2008). Advances in virtual metal forming including the ductile damage occurrence: Application to 3D sheet metal deep drawing. *J. Eng. Mater. Tech*., Vol. 130, pp. 021022-33.
12. Muscat-Fenech, C. M. & Atkins, A. G. (1994). The effect of anisotropy on fracture toughness and yield strength in the tearing of ductile sheet materials. *Int. J. Mech. Sci.*, Vol. 36, pp. 1109-1119.
13. Pimenov, A. F., Abramov, A. N., Traino, A. I. & Efremov, N. I. (1987). Reduction in strip tearing during stopping and starting of a continuous cold-rolling mill. *J. Metallurgist*, Vol. 31, pp. 94-95.
14. Lee, S. W. & Pourboghrat, F. (2005). Finite element simulation of the punchless piercing process with Lemaitre damage model. *Int. J. Mech. Sci*., Vol. 47, pp. 1756-1768.
15. Fan, J. P., Tang, C. Y., Tsui, C. P., Chan, L. C. & Lee, T. C. (2006). 3D finite element simulation of deep drawing with damage development. *Int. J. Mach. Tool Manu*., Vol. 46, pp. 1035-1044.
16. Hooputra, H., Gese, H., Dell, H. & Werner, H. (2004). A comprehensive failure model for crashworthiness simulation of aluminum extrusions. *Int. J. Crashworthiness*, Vol. 9, pp. 449–464.
17. Bai, Y., Teng, X. & Wierzbicki, T. (2009). On the application of stress triaxiality formula for plane strain fracture testing. *J. Eng. Mater. Tech*., Vol. 131, pp. 021001-10.